

Dalton Transactions

Accepted Manuscript



This is an *Accepted Manuscript*, which has been through the Royal Society of Chemistry peer review process and has been accepted for publication.

Accepted Manuscripts are published online shortly after acceptance, before technical editing, formatting and proof reading. Using this free service, authors can make their results available to the community, in citable form, before we publish the edited article. We will replace this *Accepted Manuscript* with the edited and formatted *Advance Article* as soon as it is available.

You can find more information about *Accepted Manuscripts* in the [Information for Authors](#).

Please note that technical editing may introduce minor changes to the text and/or graphics, which may alter content. The journal's standard [Terms & Conditions](#) and the [Ethical guidelines](#) still apply. In no event shall the Royal Society of Chemistry be held responsible for any errors or omissions in this *Accepted Manuscript* or any consequences arising from the use of any information it contains.



Journal Name

ARTICLE

A Family of Tetranuclear Quinolinolate Dy(III)-based Single-Molecule Magnets: Effects of Periphery Ligand Replacement on Their Magnetic Relaxation

Received 00th January 20xx,
Accepted 00th January 20xx

DOI: 10.1039/x0xx00000x

www.rsc.org/

Da Zhang,^a Yong-Mei Tian,^a Wen-Bin Sun,^{a,*} Hong-Feng Li,^a Peng Chen,^a Yi-Quan Zhang,^{b,*} and Peng-Fei Yan,^{a,*}

Three complexes with formula $\{Dy(q)_2(L)_2(u_3-OH)_2\{Dy(q)(L)_2(solvents)\}$ ($q = 8$ -quinolinolate; $L =$ Acetylacetonate (acac) and $(CH_2Cl)_2$ solvent (**1**), 1, 3-Diphenyl-1, 3-propanedione (DBM) and $(CH_2Cl)_2$ solvent (**2**), Hexafluoroacetylacetonate (hfac) and $CHCl_3$ solvent (**3**)) were structurally and magnetically characterized. They have the similar Dy_4 structural cores bridged by N and O atoms from 8-quinolinolate, and only differ in the periphery β -diketonate ligands. The variable-frequency and -temperature alternating-current (ac) magnetic susceptibility measurements reveal that complexes **1** and **2** displayed significant zero-field single-molecule-magnet (SMM) behavior, while complex **3** exhibited the field-induced SMM behavior albeit they possessed the nearly same primary coordination sphere. The ac susceptibility measurement on the diluted samples verified their relaxation of purely molecular origin and their distinct slow magnetic behaviors were related to the replacement of the periphery β -diketonate ligand, which is responsible for their different individual Dy(III) ions magnetic anisotropy and intramolecular coupling confirmed by *ab initio* calculation.

Introduction

Lanthanide-based single-molecule-magnets (SMMs) have attracted increasing attentions in recent years due to the intrinsic electronic properties of lanthanide(III) ions with large unquenched orbital moment resulting in the strong spin-orbital coupling which being along with appropriate coordination environments can lead to increased SMM performance with greater relaxation energy barriers to magnetization reversal (U_{eff}) and blocking temperature (T_B). The latter two parameters play an important role in realize their potential applications for high density information storage.¹ On the other hand, they display quantum behaviors, e.g. quantum coherence and quantum of tunneling of magnetization (QTM) etc. that leads to the potential application in molecular spintronic and quantum computing.²⁻⁴ However, the QTM is unfavourable in application of information storage targeting at high U_{eff} and T_B . To this end, generally, high magnetic anisotropy in molecule is favorable, as well as the spin dynamics related hyperfine interaction and

phonon interaction play an important role. Obviously increasing the S and retaining and aligning the high individual ions anisotropy is supposed to be an efficient strategy to enhance U_{eff} and T_B , of course it is difficult to operate, since usually increasing the S at the cost of decreasing of D .⁵ To date, the energy barriers have been reached more than 900 K while the blocking temperature was still limited 14 K⁶⁻⁸ and the fast ground state or excited state quantum of tunneling of magnetization (QTM) was considered as a major obstacle to observe slow magnetic relaxation particularly at zero field. As Dy(III) is a Kramers ion, at zero field, dipole-dipole and hyperfine interactions should be responsible for the mixing of the two Kramers ground states that allows the zero-field quantum tunneling dynamics of the magnetization and it is important challenge to overcome at the present time.⁹ In addition to the importance employment of external direct current (dc) field and enhancement of local axial symmetry to suppress QTM, the exchange coupling constant (exchange or dipole), J , must also be considered, albeit usually weak but dramatically influence the dynamic relaxation.¹⁰⁻¹² Generally, a strong exchange coupling can serve to shut down quantum tunneling processes within a single spin state manifold. In addition, for a multinuclear complex, the energetic separation between spin ground state and excited states is directly correlated to the strength of exchange coupling between paramagnetic centers.¹³ If this separation between the ground and first excited states (Δ_{diff}) is not sufficiently large, the magnetization of the molecule can undergo fast relaxation through spin excited states. As such, even an exceptionally large anisotropy barrier will not necessarily lead to a high

^a Key Laboratory of Functional Inorganic Material Chemistry Ministry of Education, Heilongjiang University No.74, Xuefu Road, Nangang District, Harbin 150080, P. R. China. E-mail: wenbinsun@126.com and yanpf@vip.sina.com

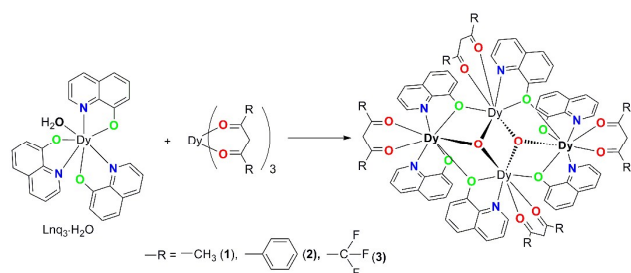
^b Jiangsu Key Laboratory for NSLSCS, School of Physical Science and Technology, Nanjing Normal University, Nanjing 210023, P. R. China. E-mail: zhangyiquan@njnu.edu.cn

† Electronic Supplementary Information (ESI) available: Additional structural, magnetic data for the complexes. CCDC 1400353, 1400355, 1400356. For ESI and crystallographic data in CIF or other electronic format see DOI: 10.1039/x0xx00000x

blocking temperature. Obviously, combination of the collection of large aligning ground spin and appropriate exchange coupling are mostly promising to improving the performance of Lanthanide-based SMMs. With this in mind, we successfully utilize the well-known 8-hydroxyquinoline (q) as bridging blocks to stabilize a series of tetranuclear Dy(III) backbone by their flexible coordination modes of N and O atoms¹⁴ and series of β -diketonate ligands were used to complete the periphery coordination sphere. The replacement on the terminal β -diketonate ligands could tune the individual local magnetic anisotropy within the tetranuclear backbone, and ultimately leads to an enhanced performance of SMM. It is interesting to note that it is rarely reported for using 8-hydroxyquinoline to build lanthanide-based SMMs,¹⁵ contrastingly to the wide researches of 8-hydroxyquinolinato-type lanthanide complexes in the field of luminescent device.¹⁶ It was also worthy learning for the further design of SMMs device, which further the prospects for single-molecule magnets, potentially bringing the goals of molecule-based information storage, quantum computing, and spin-based electronics closer to reality.

Experimental

Synthetic procedures.



Scheme 1. Synthesis of complexes 1-3.

$\text{LnL}_3(\text{H}_2\text{O})_2$ (L = β -diketonate ligands) and $\text{Lnq}_3\cdot\text{H}_2\text{O}$ were prepared by the literature procedures^{17,18}. All the other starting materials were of analytical reagent grade and were used as commercially obtained without further purification. Series of complexes abbreviated $\{\text{Dy}(\text{q})_2(\text{L})\}_2(\text{u}_3\text{-OH})_2\{\text{Dy}(\text{q})(\text{L})\}_2$ were synthesized according to a procedure previously described in the literature¹⁹ by reactions of $\text{LnL}_3(\text{H}_2\text{O})_2$ and $\text{Lnq}_3\cdot\text{H}_2\text{O}$ in a 1:1 molar ratio and the 50% diluted samples by Y(III) analogous **2a** and **2b** were synthesized by the same method. The magnetic susceptibility for complexes **1-3** were measured with a Quantum Design VSM magnetometer on polycrystalline samples. The variable-temperature magnetization was measured with an external magnetic field of 1000 Oe in the temperature range of 2–300 K. Data were corrected for the diamagnetism of the samples using Pascal constants and the sample holder by measurement.

Synthesis of $\{\{\text{Dy}(\text{q})_2(\text{acac})\}_2(\text{u}_3\text{-OH})_2\{\text{Dy}(\text{q})(\text{acac})\}_2\}\cdot(\text{CH}_2\text{Cl}_2)_2$ (**1**).

$\text{Dyq}_3\cdot\text{H}_2\text{O}$ (0.047g, 0.075mmol) and equimolar $\text{Dy}(\text{acac})_3\cdot\text{H}_2\text{O}$ (0.036g, 0.075mmol) were added to dichloromethane (30 mL) with stirring for 3 hour, giving a clear solution. After filtration,

the concentrated dichloromethane solutions were layered with n-hexane to afford the products as yellow crystals after one week. Yield: 0.062 g (75.2%). Elemental analysis (%) calcd for $\text{C}_{76}\text{H}_{70}\text{Cl}_4\text{Dy}_4\text{N}_6\text{O}_{16}$ (2115.18): C, 43.12; H, 3.31; N, 3.97. found: C,43.09 ; H, 3.27; N, 3.90.

Synthesis of $\{\{\text{Dy}(\text{q})_2(\text{DBM})\}_2(\text{u}_3\text{-OH})_2\{\text{Dy}(\text{q})(\text{DBM})\}_2\}\cdot(\text{CH}_2\text{Cl}_2)_5$ (**2**).

This complex was prepared by the same procedure as used for **1**. Yield: 0.057 g (76.3%). Elemental analysis (%) calcd for $\text{C}_{119}\text{H}_{90}\text{Cl}_{10}\text{Dy}_4\text{N}_6\text{O}_{16}$ (2864.47): C, 49.85; H, 3.14; N, 2.93. found: C,49.83; H, 3.09; N, 2.84.

Synthesis of 50% magnetically diluted sample $\{\{\text{Y}(\text{q})_2(\text{DBM})\}_2(\text{u}_3\text{-OH})_2\{\text{Dy}(\text{q})(\text{DBM})\}_2\}\cdot(\text{CH}_2\text{Cl}_2)_6$ (**2a**).

$\text{Yq}_3\cdot\text{H}_2\text{O}$ (0.027g, 0.05mmol) and equimolar $\text{Dy}(\text{DBM})_3\cdot 2\text{H}_2\text{O}$ (0.044g, 0.05mmol) were added to dichloromethane (20 mL) with stirring for half an hour, giving a clear solution. After filtration, the concentrated dichloromethane solutions were layered with n-hexane to afford the products as yellow crystals after one week. Yield: 0.053 g (74.6%). Elemental analysis (%) calcd for $\text{C}_{117}\text{H}_{86}\text{Cl}_6\text{Dy}_4\text{N}_6\text{O}_{16}$ (2694.62): C, 52.10; H, 3.19; N, 3.11. found: C, 52.09; H, 3.15 ; N, 3.04.

Synthesis of 50% magnetically diluted sample $\{\{\text{Dy}(\text{q})_2(\text{DBM})\}_2(\text{u}_3\text{-OH})_2\{\text{Y}(\text{q})(\text{DBM})\}_2\}\cdot(\text{CH}_2\text{Cl}_2)_3$ (**2b**).

$\text{Dyq}_3\cdot\text{H}_2\text{O}$ (0.031g, 0.05mmol) and equimolar $\text{Y}(\text{DBM})_3\cdot 2\text{H}_2\text{O}$ (0.040g, 0.05mmol) were added to dichloromethane (20 mL) with stirring for half an hour, giving a clear solution. After filtration, the concentrated dichloromethane solutions were layered with n-hexane to afford the products as yellow crystals after one week. Yield: 0.047 g (66.2%). Elemental analysis (%) calcd for $\text{C}_{120}\text{H}_{92}\text{Cl}_{12}\text{Dy}_4\text{N}_6\text{O}_{16}$ (2949.40): C, 48.82; H, 3.07; N, 2.84. found: C, 48.79; H, 3.03; N, 2.78.

Synthesis of $\{\{\text{Dy}(\text{q})_2(\text{hfac})\}_2(\text{u}_3\text{-OH})_2\{\text{Dy}(\text{q})(\text{hfac})\}_2\}\cdot\text{CHCl}_3$ (**3**).

This compound was prepared by the same procedure as used for **2**. Yield: 0.101 g (69.8%). Elemental analysis (%) calcd for $\text{C}_{75}\text{H}_{43}\text{Cl}_3\text{Dy}_4\text{F}_{24}\text{N}_6\text{O}_{16}$ (2496.50): C, 36.05; H, 1.72; N, 3.36. found: C, 36.03; H, 1.68; N, 3.29.

Table 1. Crystal data for complexes 1–3.

	1	2	3
Empirical formula	C ₇₆ H ₇₀ Cl ₄ Dy ₄ N ₆	C ₁₁₉ H ₉₀ Cl ₁₀ Dy ₄ N	C ₇₅ H ₄₃ Cl ₃ Dy ₄ F ₂₄
FW (g.mol ⁻¹)	2115.18	2864.47	2496.50
Crystal system	monoclinic	triclinic	monoclinic
Space group	P2 ₁ /c	P-1	P2 ₁ /n
T (K)	293(2)	293(2)	293(2)
a (Å)	12.1469(5)	13.9004(5)	13.1652(2)
b (Å)	24.8920(10)	15.1696(6)	24.7100(3)
c (Å)	13.3583(6)	16.5072(6)	13.1956(3)
α (°)	90	110.993(4)	90
β (°)	106.209(4)	104.394(3)	101.6242(18)
γ (°)	90	106.271(3)	90
V (Å ³)	3878.5(3)	2873.37(19)	4204.65(13)
pcacd (Mg.m ⁻³)	1.811	1.655	1.972
μ (mm ⁻¹)	4.015	2.869	3.729
F(000)	2056	1408	2388
Collected reflections	23054	23048	38878
Independent reflections	7922	12905	10078
Rint	0.1011	0.0448	0.0284
R1 [I > 2σ(I)]	0.0475	0.0427	0.0259
wR2 (all data)	0.1071	0.1084	0.0624
GOF	1.022	1.048	1.031

X-ray Crystallography. Diffraction intensity data for single crystals of complexes were collected with a Rigaku R-Axis RAPID imaging-plate X-ray diffractometer at 293 K (an Xcalibur, Eos diffractometer using graphite-monochromated Mo-K α radiation). The structures were solved by direct methods and refined by the full-matrix least-squares on F^2 using the SHELXTL-97 software package.²⁰ All non-hydrogen atoms were refined with isomorphous displacement parameters. The crystallographic data for 1–3 are listed in Table 1, and additional crystallographic information is available in the Supporting Information.

Results and discussion

Structural descriptions of complexes 1–3.

Single-crystal X-ray diffraction studies indicate that complex 2 crystallizes in the triclinic space group P-1, whereas complex 1 crystallizes in the monoclinic space group P2₁/c and complex 3 crystallizes in the monoclinic space group P2₁/n. The complexes 1–3, 2a and 2b have similar framework structure, only with small different in the substituent group of β-diketonate backbone (Scheme 1 and Fig. S2, S12, Supporting Information). The structure of 1 will be described as representative of the whole series. Details for the structure solution and refinement are summarized in Table 1. Moreover, for complexes 1–3, the coordination geometry of Dy(III) ions were calculated by utilizing the SHAPE 2.1 software²¹ (Table S1 in Supporting Information). A summary of important selected interatomic distances of complexes 1–3 are listed in Supporting Information, Table S2 and Table S3.

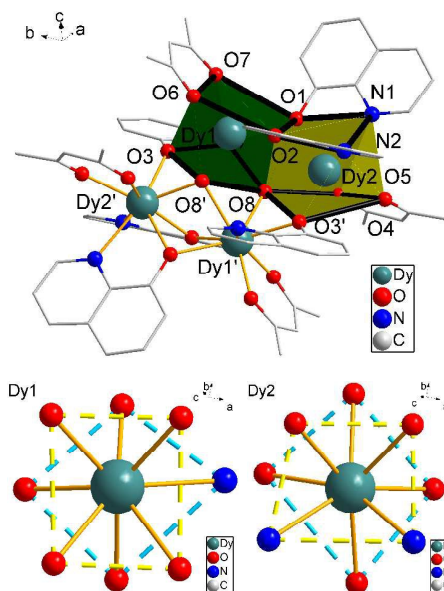


Fig. 1 Polyhedral representation of the face sharing successive polyhedra of 1 (top); Distorted square-antiprism geometry around Dy1 (bottom left) and Dy2 (bottom right), unnecessary atoms are omitted for clarity.

The partially labeled molecular structure of complex 1 is presented in Fig. 1a. As we can see, Dy1 is eight-coordinated environment comprising N and O atoms from one acac, two chelating 8-hydroxyquinolinato, one μ-phenoxo of 8-hydroxyquinolinato, and one μ₃-OH⁻, and results in a square antiprism coordination geometry surrounding Dy1. Dy2 is also eight-coordinated by one acac, but one chelating 8-hydroxyquinolinato, two μ-phenoxo of 8-hydroxyquinolinato, and two μ₃-OH⁻, also leads to a distorted square-antiprism coordination geometry.

The distortion is visualized by continuous shape measures performed with SHAPE 2.1, which give the parameters based on the ideal square-antiprism for Dy1, 0.968 for 1, 0.900 for 2 and 0.668 for 3, the larger parameters indicates the more distortion from the ideal geometry. For Dy2, 1.425 for 1, 1.111 for 2 and 0.936 for 3. The coordination polyhedron of Dy1 in 1 and 2 is slightly more symmetric than that of Dy2, whereas the coordination polyhedron of Dy1 is less symmetric compared with that of Dy2 in 3.

It is also worth noting that the distances of Dy-O and Dy1-Dy2 are dependent on the different steric hindrance effects with electron withdrawing or donating substituents on the periphery β-diketonate ligands, which might lead to different local symmetry and strength of ligand field and even the intramolecular magnetic interaction²². The average distances of Dy-O (β-diketonate) in 1, 2 and 3 are 2.3070, 2.3115, 2.3605 Å, respectively. Complex 3 has the shortest distances of Dy1-Dy2 (3.4936(2) Å) and Dy1-Dy2' (3.8172(4) Å) due to strong electron withdrawing capability of fluoride in hfac⁻¹, the distances of Dy1-Dy2 (3.5583(4) Å) and Dy1-Dy2' (3.8531(4) Å) in complex 2 are longer than complex 3.

Magnetic Properties

The static magnetic measurements were performed on the polycrystalline samples using a Quantum Design VSM

superconducting quantum interference device (SQUID) magnetometer. The temperature dependence of magnetic susceptibility $\chi_M T$ for complexes **1-3** is shown in Fig. 2.

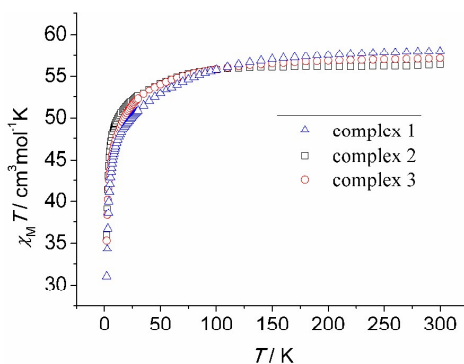


Fig. 2 Temperature-dependent $\chi_M T$ products under 1000 Oe for complexes **1**, **2** and **3**.

The values of $\chi_M T$ are 58.02, 56.41, and 57.17 $\text{cm}^3 \cdot \text{K} \cdot \text{mol}^{-1}$ at 300K for complexes **1**, **2**, and **3**, respectively, which are in good agreement with the theoretical value of 56.68 $\text{cm}^3 \cdot \text{K} \cdot \text{mol}^{-1}$ for four isolated Dy(III) ions ($^6\text{H}_{15/2}$, $S = 5/2$, $L = 5$, $g = 4/3$, $\chi_M T = 14.17 \text{ cm}^3 \cdot \text{K} \cdot \text{mol}^{-1}$). On lowering the temperature, the $\chi_M T$ product decreases gradually and more rapidly below 50 K and reaches 31.06, 35.95, and 35.32 $\text{cm}^3 \cdot \text{K} \cdot \text{mol}^{-1}$, respectively at 1.8 K, which is likely due to thermal depopulation of Stark sublevels and the possible antiferromagnetic intramolecular Dy-Dy interaction or dipole-dipole interaction between the molecules. The magnetization of **1-3** from zero to 70 kOe dc field at 2, 3, 5 and 8 K are shown in Fig. S3, Supporting Information. The magnetization measurements for complexes **1-3** (Fig. S3) show a relatively rapid increase below 1 T and slow linear increase without complete saturation up to 7 T. Their magnetization values (22.35, 23.24 and 24.51 N β) are lower than their theoretically derived values 40.00 N β . As aforementioned, the complexes may have low-lying excited states or significant magnetic anisotropy resulting in large differences between experimental and theoretical values. Further confirmation was obtained with the M vs H/T plots (Fig. S3, inset, Supporting Information), since all curves were not superimposed on a single master curve as expected for an isotropic system with a well-defined ground state we can conclude the presence of low-lying excited states or significant magnetic anisotropy.

In order to probe the magnetic dynamic behavior of these complexes, the ac susceptibilities at various frequencies and temperatures in the absence of dc field are measured and depicted in Fig. 3 and Fig. S8-S9. The out-of-phase (χ'') susceptibilities show significant frequency dependence peaks at about 10 K for complexes **1** and **2** (Fig. 3), which clearly indicates the slow relaxation of magnetization arises from SMM properties. The maximum peaks of the out-of-phase signals were found from 7 K to 12 K for an oscillating field range of 1 Hz to 1000 Hz. The first and clear peaks are observed at 100 and 325 Hz for complexes **1** and **2** respectively.

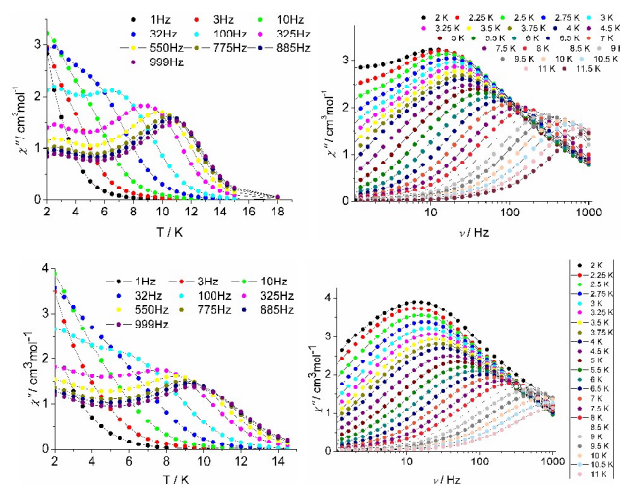


Fig. 3 Temperature dependence of the out-of-phase (χ'') ac susceptibility signals (left) and frequency dependence of the out-of-phase (χ'') ac susceptibility signals (right) for complexes **1** (top) and **2** (bottom) under zero-dc field.

The increasing of χ' and χ'' below 7 K is indicative of the quantum tunneling of the magnetization (QTM) at a zero dc field. In the frequency dependent susceptibility measurements, temperature independent peaks in the low temperature range were observed (Fig. 3), which further proved the occurrence of a resonant QTM process. To confirm whether the relaxation in **1** and **2** is thermally activated mechanism, the natural log of the relaxations, τ extracted from the peak maxima of χ'' , were plotted versus $1/T$ to check for Arrhenius-type linearity which was normally referred to the Orbach relaxation of the magnetization ($\tau = \tau_0 \exp(U_{\text{eff}}/K_B T)$, Fig. 4). It is interesting to note that, the curvature in the $\ln(\tau)$ versus $1/T$ plot under zero field was observed for **1** and **2**, and the QTM process was usually responsible for this deviation from Arrhenius-type linearity. Owing to the Kramers nature of Dy(III) ion, at zero field, the weak intramolecular coupling, dipole-dipole and hyperfine interactions should be responsible for the mixing of the two Kramers ground states that allows the zero-field quantum tunneling dynamics of the magnetization. To suppress the QTM effect, ac susceptibility measurements were performed under optimum static dc field of 600 and 1500 Oe for complexes **1** and **2**, respectively (Fig. S6-S7). The optimum field was selected by determining which field was able to slow the frequency dependent χ'' maxima to the slowest relaxation rate (Fig. S4-S5). It does efficiently suppress the QTM process with the diminishing χ'' signals at the low temperature range (Fig. S7). It is also noteworthy that the plots of $\ln(\tau)$ versus $1/T$ either under optimum static dc field still exhibit obvious curvature which indicates perhaps other relaxation pathway is also operative (Fig. 4). The presence of multiple relaxation processes is possible as reported in a few SIMs.²³⁻²⁶ In view of this, we fitted the magnetic data with the equation 1 considering the spin-lattice relaxation of both Raman and Orbach processes.²⁷

$$1/\tau = C T^n + \tau_0^{-1} \exp(-U_{\text{eff}}/K_B T) \quad (1)$$

The first and second terms correspond to the Raman and Orbach processes, respectively. In general, $n = 9$ is rational for Kramers ions, but when both the acoustic and optical phonons

are considered depending on the structure of energy levels, n values between 1 and 6 are reasonable.²⁸ Equation 1 affords $n = 1.2$, $U_{\text{eff}}/K_{\text{B}} = 50$ K, $\tau_0 = 2.7 \times 10^{-6}$ s in the absence of dc field, $n = 2.5$, $U_{\text{eff}}/K_{\text{B}} = 64$ K, $\tau_0 = 9.6 \times 10^{-7}$ s under 600 Oe dc field for **1**, and $n = 1.5$, $U_{\text{eff}}/K_{\text{B}} = 46$ K, $\tau_0 = 2.6 \times 10^{-6}$ s in the absence of dc field, $n = 2.9$, $U_{\text{eff}}/K_{\text{B}} = 71$ K, $\tau_0 = 3.7 \times 10^{-7}$ s under 1500 Oe dc field for **2**, respectively (Fig. 4). These values are in good agreement with the ones extracted from the linear section of the Arrhenius plot of $\ln(\tau)$ versus $1/T$ ($U_{\text{eff}}/K_{\text{B}} = 52$ K, $U_{\text{eff}}/K_{\text{B}} = 41$ K in zero dc field for **1** and **2**, respectively.), which describes a region where the relaxation is a thermally activated process.

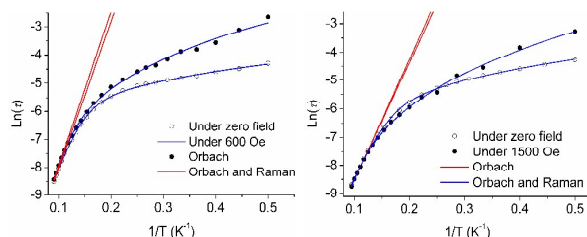


Fig. 4 Plots of $\ln(\tau)$ versus $1/T$ at zero, 600 Oe dc field for **1** (left) and at zero, 1500 Oe for **2** (right). The blue solid lines represent the fitting of the frequency-dependent data by Equation 1 for **1** and **2**, and the red solid lines represent the pure Arrhenius fitting at the high-temperature linear region for **1** and **2**.

Whereas only increasing frequency-dependent signals were observed in the χ'' vs T plot (Fig. 5) for complex **3** in the absence of dc field, and the relaxation barriers cannot be extracted from the χ'' vs ν plot as no full peak was observed in zero dc field even under a 1500 dc field. The observation indicates a more pronounced QTM operates in **3** than **1** and **2** albeit they visually possessed nearly same Dy4 cores.

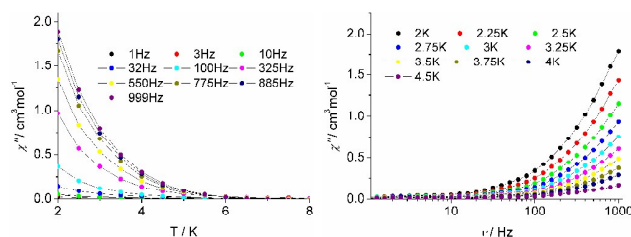


Fig. 5 Temperature dependence of the out-of-phase (χ'') ac susceptibility signals (left) and frequency dependence of the out-of-phase (χ'') ac susceptibility signals (right) for complex **3** under zero-dc field.

To probe the origin of slow magnetic relaxation, ac susceptibility measurement for diluted samples of **2** denoted as **2a** and **2b** was carried out (Fig. S12). Their nearly identical χ'' peaks under same frequency indicate the same relaxation source compared with **2**, which arises from the molecular origin. It is interesting to note that the more pronounced increasing χ'' signals at low temperature region compared with the undiluted sample **2** were observed (Fig. S14). This is most likely due to most Dy(III) ions sites were replaced by dimagnetic Y(III) ions within the diluted samples and where the single Dy(III) ions magnetic anisotropy became prominent, in which the QTM is commonly pronounced accompany with increasing χ'' signals and similar phenomenon was found in some lanthanide-based dinuclear SMMs²⁹. The close energy barriers compared with **2** were extracted as $U_{\text{eff}}/K_{\text{B}} = 39$ K, $\tau_0 =$

3.9×10^{-6} s, $U_{\text{eff}}/K_{\text{B}} = 39$ K, $\tau_0 = 3.7 \times 10^{-6}$ s by fitting $\ln(\tau)$ versus $1/T$ (Fig. S17), and the rate of QTM in **2a** and **2b** were significant faster than that of **2** from the $\ln(\tau)$ versus $1/T$ plot (Fig. S18). Although there are two slightly different coordination geometry of Dy1 and Dy2 in complexes **1** and **2**, only single peaks of the temperature and frequency dependent χ'' signals were observed, which is possibly due to the very close coordination geometry between the two Dy(III) ions in molecule as structural description above. The graphical representation of χ'' vs χ' (cole-cole plots³⁰) in the temperature range 5-11.5K and 5.5-11K for **1** and **2** respectively further confirmed these single relaxation processes (Fig. S24). This fit provides a value for the parameter α , which is related to the width of the distribution of relaxation times, i.e. $\alpha = 1$ corresponds to an infinitely wide distribution of relaxation times, whereas $\alpha = 0$ represents a single relaxation process. We obtained a value for α in the range 0.03-0.3 and 0.07-0.3 for **1** and **2** respectively, revealing a narrow to moderate distribution of relaxation times (Table S4-S5). For temperatures below 5 K, however, the data can not be fitted very well via using a generalized Debye model^{31,32} or the sum of two modified Debye functions, which is most likely due to admixing other relaxations like QTM and/or Raman processes.

The above observations indicate complexes **3**, compared with **1** and **2**, displayed significant different dynamic relaxations, which is mostly related with the changes in the local coordination environment of Dy(III) ion. To probe the divergence between **1**, **2** and **3**, further insight into the electronic structure and magnetic anisotropy in the investigated dysprosium complexes was obtained by ab initio calculations. Complete-active-space self-consistent field (CASSCF) calculations on two types of individual Dy(III) fragments for each of complexes **1-3** on the basis of X-ray determined geometries have been carried out with MOLCAS 7.8³³ and SINGLE_ANISO³⁴ programs (see Supporting Information for details). The lowest spin-orbit energies and the corresponding g tensors of complexes **1-3** are shown in Table S6. Moreover, from Table S6, the energy separations (Δ_{diff}) between the ground and the first Kramers doublets for the Dy(III) fragments of **1-3** are apparently deviated from the extracted experimental energy barriers. Normally, the Δ_{diff} is related with the thermally activated relaxation barrier through the first excited state i.e. Orbach mechanism. Generally, the computed values are overestimating the U_{eff} values and the discrepancy between computed (U_{calcd}) and the experimental (U_{eff}) values are expected as the computed values assume inherently no QTM between the ground-state KDs and no intermolecular interactions or no vibronic coupling these are conditions that are very stringent and difficult to meet and not considered in the U_{calcd} values.³⁵

The magnetic susceptibilities of complexes **1-3** have been simulated with the program POLY_ANISO³⁶ (see Fig. S27) using the exchange parameters from Table S7.

All parameters from Table S7 were calculated with respect to the pseudo spin $\tilde{S} = 1/2$ of the Dy(III) ions. For complex **1**, the total coupling parameters J (dipolar and exchange) were included into fit the magnetic susceptibilities. The calculated

and experimental $\chi_M T$ versus T plots of complexes **1-3** are shown in Fig. S27, where the fit is very close to the experimental data in the whole temperature regime for each of them. From Table S7, the Dy(III)-Dy(III) interactions in three complexes are all very small, and only the ferromagnetic exchange coupling J_3 in complex **2** is the strongest. The main magnetic axes on two Dy(III) were indicated in Fig. S26 where the magnetic axes on the two types of Dy(III) for each complex have some differences (Table S 8). The strongest bonds between the metal center and the coordinated atoms may favors an axial nature of the ligand field and thus influences the single-ion anisotropy³⁷. In this case, the easy axis in **1**, **2** and **3** are consistent with the bonds between metal center and the O atoms of β -diketonate ligands (Fig. S26, Table S2).

The weak intramolecular coupling most likely leads to a negligible effect on its dynamic behavior. Therefore the different substituents on the β -diketonate terminal become a key factor to cause the lowest spin-orbit energies and easy axis difference. Angles between easy axis on Dy1 and Dy2 in **3** (25.0°) are smaller than **1** (40.6°) and **2** (40.0°), additionally the angles between easy axis on individual Dy(III) ions and Dy1-Dy2 have the same trends. The non-collinear arrangement of the local magnetic axes with respect to each other and to the Dy-Dy axis does not favor strong dipolar magnetic interaction³⁷ and is often detrimental to the performance of Dy(III) SMMs, in the present case, which is mostly due to the different substituents on the β -diketonate terminal that ultimately impact on the the dynamic relaxation of SMMs.

Conclusions

A series of planar tetranuclear Dy(III) SMMs were prepared as well as characterized structurally and magnetically. The structural analyses demonstrated that the use of 8-hydroxyquinolinato and β -diketonate ligands is ideal for isolation of planar tetranuclear lanthanide clusters. In our case, the intramolecular coupling is weak and possibly have a negligible impact on the dynamic relaxation, however, the effects of the replacement to the periphery terminal ligands on their magnetic relaxation are obvious, which reveals the feasibility to modulate the magnetic anisotropy of multinuclear SMMs by fine-tuning the local coordination environment albeit beyond the first coordination sphere.

Acknowledgements

This work was supported by the NSFC (no. 21572048, 21102039, 51302068, 21272061, 51102081, and 21302045), the Educational Commission of Heilongjiang Province (1254G045, 12541639) Natural Science Foundation of Jiangsu Province of China (BK20151542) and the Priority Academic Program Development of Jiangsu Higher Education Institutions.

Notes and references

- (a) R. Sessoli, D. Gatteschi, A. Caneschi, M. A. Novak, *Nature*, 1993, **365**, 141; (b) R. Sessoli, H. L. Tsai, A. R. Schake, S. Wang, J. B. Vincent, K. Folting, D. Gatteschi, G. Christou, D. N. Hendrickson, *J. Am. Chem. Soc.*, 1993, **115**, 1804.
- (a) L. Bogani, W. Wernsdorfer, *Nat. Mater.*, 2008, **7**, 179; (b) J. R. Friedman, M. P. Sarachik, J. Tejada, R. Ziolo, *Phys. Rev. Lett.*, 1996, **76**, 3830; (c) L. Thomas, F. Lioni, R. Ballou, D. Gatteschi, R. Sessoli, B. Barbara, *Nature*, 1996, **383**, 145; (d) W. Wernsdorfer, R. Sessoli, *Science*, 1999, **284**, 133; (e) S. Sanvito, *Chem. Soc. Rev.*, 2011, **40**, 3336.
- (a) M. N. Leuenberger, D. Loss, *Nature*, 2001, **410**, 789; (b) D. Gatteschi, R. Sessoli, *Angew. Chem. Int. Ed.*, 2003, **42**, 268; (c) G. Aromi, D. Aguilu, P. Gamez, F. Luis, O. Roubeau, *Chem. Soc. Rev.*, 2012, **41**, 537; (d) S. Gao, *Molecular Nanomagnets and Related Phenomena, Structure and Bonding*, Springer Berlin Heidelberg press, 2015, **164**
- A. Caneschi, D. Gatteschi, R. Sessoli, A. L. Barra, L. C. Brunel, M. Guillot, *J. Am. Chem. Soc.*, 1991, **113**, 5873.
- (a) E. Ruiz, J. Cirera, J. Cano, S. Alvarez, C. Loose, J. Kortus, *Chem. Commun.*, 2008, **1**, 52; (b) Y. N. Guo, L. Ungur, G. E. Granroth, A. K. Powell, C. Wu, S. E. Nagler, J. K. Tang, L. F. Chibotaru, D. M. Cui, *Sci. Rep.* 2014, **4**, 5471.
- C. R. Ganivet, B. Ballesteros, de la G. Torre, J. M. Clemente-Juan, E. Coronado, T. Torres, *Chem. Eur. J.*, 2013, **19**, 1457.
- R. J. Blagg, L. Ungur, F. Tuna, J. Speak, P. Comar, D. Collison, W. Wernsdorfer, E. J. L. McInnes, L. F. Chibotaru, R. E. P. Winpenny, *Nat. Chem.*, 2013, **5**, 673.
- J. D. Rinehart, M. Fang, W. J. Evans, J. R. Long, *J. Am. Chem. Soc.*, 2011, **133**, 14236.
- (a) D. N. Woodruff, R. E. P. Winpenny, R. A. Layfield, *Chem. Rev.*, 2013, **113**, 5110; (b) H. L. C. Feltham, S. Brooker, *Coord. Chem. Rev.*, 2014, **276**, 1; (c) S. Demir, Ie-R. Jeon, J. R. Long, T. D. Harris, *Coord. Chem. Rev.*, 2015, **289-290**, 149; (d) L. Ungur, S. Y. Lin, J. K. Tang, L. F. Chibotaru, *Chem. Soc. Rev.*, 2014, **43**, 6894; (e) J. K. Tang, P. Zhang, *Lanthanide Single Molecule Magnets*, Springer Berlin Heidelberg press, 2015.
- S. F. Xue, Y. N. Guo, L. Ungur, J. K. Tang, L. F. Chibotaru, *Chem. Eur. J.*, 2015, **21**, 1.
- F. Habib, M. Murugesu, *Chem. Soc. Rev.*, 2013, **42**, 3278.
- S. Demir, M. Nippe, M. I. Gonzalez, J. R. Long, *Chem. Sci.*, 2014, **5**, 4701.
- Ie-R. Jeon, J. G. Park, D. J. Xiao, T. D. Harris, *J. Am. Chem. Soc.*, 2013, **135**, 16845.
- C. W. Tang, S. A. VanSlyke, *Appl. Phys. Lett.*, 1987, **51**, 913.
- (a) N. F. Chilton, G. B. Deacon, O. Gazukin, P. C. Junk, B. Kersting, S. K. Langley, B. Moubarak, K. S. Murray, F. Schleife, M. Shome, D. R. Turner, J. A. Walker, *Inorg. Chem.*, 2014, **53**, 2528; (b) E. M. Pineda, N. F. Chilton, R. Marx, M. Dörfel, D. O. Sells, P. Neugebauer, S. -D. Jiang, D. Collison, J. V. Slageren, E. J. L. McInnes, R. E. P. Winpenny, *Nat. Commun.*, 2014, **5**, 5243; (c) F. Z. Duan, L. Z. Liu, C. Y. Qiao, H. M. Yang, *Inorg. Chem. Commun.*, 2015, **55**, 120.
- (a) N. M. Shavaleev, R. Scopelliti, F. Gumy, J. -C. G. Bünzli, *Inorg. Chem.*, 2008, **47**, 9055; (b) H. B. Xu, Y. T. Zhong, W. X. Zhang, Z. N. Chen, X. M. Chen, *Dalton Trans.*, 2010, **39**, 5676.
- (a) Y. Hasegawa, Y. Kimura, K. Murakoshi, Y. Wada, J. -H. Kim, N. Nakashima, T. Yamanaka, S. J. Yanagida, *Phys. Chem.*, 1996, **100**, 10201; (b) H. Bauer, J. Blanc, D. L. Ross, *J. Am. Chem. Soc.*, 1964, **86**, 5125.
- (a) O. M. Khreis, W. P. Gillin, M. Somerton, R. J. Curry, *Org. Electron.*, 2001, **2**, 45; (b) J. Thompson, R. I. R. Blyth, G. Gigli, R. Cingolani, *Adv. Funct. Mater.*, 2004, **14**, 979.
- H. B. Xu, J. G. Deng, L. Y. Zhang, Z. N. Chen, *Cryst. Growth Des.*, 2013, **13**, 849.
- G. M. Sheldrick, SHELXL-97, Program for X-ray Crystal Structure Refinement, University of Göttingen, Göttingen, Germany, 1997.

Journal Name ARTICLE

- 21 M. Llunell, D. Casanova, J. Cirera, P. Alemany, S. Alvarez, SHAPE, v2.1; University of Barcelona and The Hebrew University of Jerusalem, Barcelona and Jerusalem, 2013.
- 22 F. Habib, G. Brunet, V. Vieru, I. Korobkov, L. F. Chibotaru, M. Murugesu, *J. Am. Chem. Soc.*, 2013, **135**, 13242.
- 23 S. Titos-Padilla, J. Ruiz, J. M. Herrera, E. K. Brechin, W. Wernsdorfer, F. Lloret, E. Colacio, *Inorg. Chem.*, 2013, **52**, 9620.
- 24 J. L. Liu, K. Yuan, J. D. Leng, L. Ungur, W. Wernsdorfer, F. S. Guo, L. F. Chibotaru, M. L. Tong, *Inorg. Chem.*, 2012, **51**, 8538.
- 25 E. Colacio, J. Ruiz, E. Ruiz, E. Cremades, J. Krzystek, S. Carretta, J. Cano, T. Guidi, W. Wernsdorfer, E. K. Brechin, *Angew. Chem. Int. Ed.*, 2013, **52**, 9130.
- 26 W. B. Sun, B. Yan, Y. Q. Zhang, B. W. Wang, Z. M. Wang, J. H. Jia, S. Gao, *Inorg. Chem. Front.*, 2014, **1**, 503.
- 27 A. Abragam, B. Bleaney, *Electron Paramagnetic Resonance of Transition Ions*; Clarendon Press: Oxford, U.K., 1970.
- 28 K. N. Shirivastava, *Phys. Status Solidi B*, 1983, **117**, 437.
- 29 F. Habib, P. H. Lin, J. Long, I. Korobkov, W. Wernsdorfer, M. Murugesu, *J. Am. Chem. Soc.*, 2011, **133**, 8830.
- 30 (a) K. S. Cole and R. H. J. Cole, *Chem. Soc.*, 1941, **9**, 341; (b) S. M. J. Aubin, Z. Sun, L. Pardi, J. Krzystek, K. Folting, L. J. Brunel, A. L. Rheingold, G. Christou and D. N. Hendrickson, *Inorg. Chem.*, 1999, **38**, 5329.
- 31 D. Gatteschi, R. Sessoli and J. Villain, *Molecular Nanomagnets*, Oxford University Press: New York, 2006 and references therein.
- 32 J. Long, F. Habib, P.-H. Lin, I. Korobkov, G. Enright, L. Ungur, W. Wernsdorfer, L. F. Chibotaru and M. Murugesu, *J. Am. Chem. Soc.*, 2011, **133**, 5319.
- 33 G. Karlström, R. Lindh, P. -A. Malmqvist, B. O. Roos, U. Ryde, V. Veryazov, P. -O. Widmark, M. Cossi, B. Schimmelpfennig, P. Neogrady, L. Seijo, *Comput. Mater. Sci.*, 2003, **28**, 222.
- 34 (a) L. F. Chibotaru, L. Ungur, A. Soncini, *Angew. Chem. Int. Ed.*, 2008, **47**, 4126; (b) L. Ungur, W. Van den Heuvel, L. F. Chibotaru, *New J. Chem.*, 2009, **33**, 1224; (c) L. F. Chibotaru, L. Ungur, C. Aronica, H. Elmoll, G. Pilet, D. Luneau, *J. Am. Chem. Soc.*, 2008, **130**, 12445.
- 35 (a) L. Ungur, L. F. Chibotaru, *Phys. Chem. Chem. Phys.*, 2011, **13**, 20086; (b) D. Aravena, E. Ruiz, *Inorg. Chem.*, 2013, **52**, 13770; (c) J. M. Zadrozny, M. Atanasov, A. M. Bryan, C. Y. Lin, B. D. Rekker, P. P. Power, F. Neese, J. R. Long, *Chem. Sci.*, 2013, **4**, 125; (d) M. Atanasov, J. M. Zadrozny, J. R. Long, F. Neese, *Chem. Sci.*, 2013, **4**, 139; (e) W. B. Sun, P. F. Yan, Sh. D. Jiang, B. W. Wang, Y. Q. Zhang, H. Fe. Li, P. Chen, Z. M. Wang, S. Gao, *Chem. Sci.*, 2015, DOI: 10.1039/c5sc02986d.
- 36 S. K. Langley, D. P. Wielechowski, V. Vieru, N. F. Chilton, B. Moubaraki, B. F. Abrahams, L. F. Chibotaru, K. S. Murray, *Angew. Chem. Int. Ed.*, 2013, **52**, 12014.
- 37 S. F. Xue, Y. N. Guo, L. Ungur, J. K. Tang, L. F. Chibotaru, *Chem. Eur. J.*, 2015, **21**, 14099.